Environ. Sci. Technol. **1999**, *33,* 3140−3144

The Link between Clay Mineral Weathering and the Stabilization of Ni Surface Precipitates

ROBERT G. FORD,*,† ANDREAS C. SCHEINOST, KIRK G. SCHECKEL, AND DONALD L. SPARKS

Department of Plant and Soil Sciences, University of Delaware, Newark, Delaware 19717

The formation of transition-metal surface precipitates may occur during sorption to clay minerals under ambient soil conditions. This process may lead to significant long-term stabilization of the metal within the soil profile. However, the rates and mechanisms controlling surface precipitate formation are poorly understood. We monitored changes in the reversibility of Ni sorbed to a clay mineral, pyrophyllite, in model batch experiments maintained at pH 7.5 for up to 1 year. The macroscopic sorption and dissolution study was complemented by a time-resolved characterization of the sorbed phase via spectroscopic and thermal methods. We found that nickel became increasingly resistant, over time, to extraction with EDTA. Initially, the sorbed phase consisted of a Ni−Al layered double hydroxide (LDH). With time, the anionic species in the interlayer space of the LDH changed from nitrate to silica polymers transforming the LDH gradually into a precursor Ni−Al phyllosilicate. We believe that this phase transformation is responsible for a substantial part of the observed increase in dissolution resistance. Thus, clay mineral weathering and the time-dependent release of Al and Si ions controlled Ni precipitate nucleation and transformation. Our results suggest a potential pathway for long-term Ni stabilization in soil.

Introduction

The mobility and bioavailability of metals in soil is mediated by sorption reactions at the mineral−water interface (*1, 2*). Quantification of metal speciation at the mineral surface is a necessary step for assessing the toxicity of metals in the environment. Past research has focused on the development of surface complexation models (SCMs) to aid in speciation of metal sorption (*3*). Implicit to most SCMs is the assumption that the sorbent surface is in equilibrium with the soil solution and functions solely as a reservoir of reactive sites for ion sorption. Studies of Co and Ni sorption to Al-bearing oxide minerals, however, have shown that sorbent surfaces dynamically alter in response to chemical perturbations at the mineral−water interface resulting in the release of Al lattice ions that coprecipitate with the sorbate (*4*−*7*). In these systems, precipitation effectively competes with adsorption reactions (*8*).

* Corresponding author phone: (580)436−8872; fax: (580)436−8703; e-mail: ford.robert@epa.gov.

† Current address: Robert S. Kerr Environmental Research Center, U.S. EPA, P.O. Box 1198, Ada, OK 74820.

The suggested precipitate phase shares structural features common to the hydrotalcite group of minerals and the layered double hydroxides (LDH) observed in catalyst synthesis (*9, 10*). The LDH structure is built up of stacked sheets of edge-sharing metal octahedra separated by anions between the interlayer spaces. The general structural formula can be expressed as $[Me^{2+}_{1-x}Me^{3+}_{x}(OH)_2]^{x+}\cdot(x/n)A^{n-}\cdot mH_2O$ where the presence of interlayer anions, A^{n-}, is required to compensate the excess positive charge imparted by Al^{3+} substitution into the octahedral layer.

Scheidegger et al. (*11*) hypothesized that the Al^{3+} required for Ni−Al LDH formation was derived from weathering of the clay mineral surface. A time-dependent extended X-ray absorption fine structure (EXAFS) study showed a continuous increase in the Ni−Ni coordination number, which may be related to structural transformations occurring within the surface precipitate over a period of 3 months (*7*). The mechanism(s) responsible for these changes remains elusive, however, since analysis of second-shell contributions from light elements, e.g., Al and Si, is poorly constrained in the hard X-ray region (*12*). We anticipate that these structural changes could lead to a significant change in the stability of sorbed nickel. Insufficient understanding of the mechanisms controlling the nucleation and transformation of surface precipitates at the mineral−water interface severely limits prediction of metal partitioning in environmental systems. Thus, we employed a multimethod approach to elucidate the solid-state processes controlling the long-term sequestration of Ni to a clay mineral surface.

Experimental Methods

Ni Sorption−Desorption. Nickel sorption to the $<2\,\mu$m size fraction of pyrophyllite was carried out at pH 7.5 and 0.1 M $NaNO_3$ in batch aqueous systems. A Ni-to-solids ratio of 0.3 mmol g^{-1} was employed using either a 5 or 10 g L^{-1} pyrophyllite concentration. Nickel sorption as a function of time was determined by measuring aqueous Ni by inductively coupled plasma emission spectroscopy (ICP). The pH of replicate experimental systems was controlled by two different methods: (1) through use of an automatic pH stat for the first 3 days followed by daily manual additions of 0.1 M NaOH or (2) through addition of 50 mM 4-(2-hydroxyethyl)-1-piperazineethanesulfonic acid (HEPES). Base additions, and the potential for local oversaturation with respect to $Ni(OH)_2$, were avoided in the HEPES buffered systems. Previous studies indicate that HEPES does not significantly interfere with Ni sorption to mineral surfaces (*13*). Both approaches to buffer pH were employed to remain consistent with previous studies (*11*) and to characterize the potential for oversaturation artifacts. However, comparison of the rates of Ni sorption and the speciation of the Ni sorption product indicated that homogeneous precipitation of $Ni(OH)_2$ did not occur.

The reversibility of sorbed/precipitated Ni was assessed by EDTA extraction. Nickel-reacted pyrophyllite (300 mg) was suspended in 30 mL of a 1 mM EDTA solution at pH 7.5 for 24 h. The suspension was centrifuged at 15 000 rpm for 4 min, the supernatant was decanted, and fresh EDTA solution was added to the remaining solids. The extraction was repeated 10 times, and dissolved Ni was determined by ICP. This procedure was employed to monitor relative changes in the extractability of Ni as a function of aging time. EDTA forms a stable Ni solution complex, and previous studies have shown that EDTA promotes desorption of Ni sorbed to oxide surfaces and the dissolution of poorly crystalline oxide phases (*14*−*16*).

10.1021/es990271d CCC: $18.00 © 1999 American Chemical Society
Published on Web 08/05/1999

Characterization of Solid-Phase Ni. The nickel surface precipitate that formed on pyrophyllite was characterized by diffuse reflectance spectroscopy (DRS), high-resolution thermogravimetric analysis (HRTGA), and extended X-ray absorption spectroscopy (EXAFS). Diffuse reflectance spectra were collected with a Perkin-Elmer Lambda 9 spectrophotometer equipped with a 5-cm Spectralon-coated integrating sphere over the wavelength range 500−1000 nm. The ν_2 absorption band was extracted from the raw spectra by ratioing the diffuse reflectance spectra of the samples and references to the spectrum of unreacted pyrophyllite (*7*). Approximately 15−20 mg was analyzed by HRTGA under a N_2 atmosphere with a TA Instruments 2950 HiRes Thermogravimetric analyzer (instrument settings: 20 °C min^{-1}, resolution = 5.0, sensitivity = 1.0). X-ray absorption spectra at the Ni−Kα edge were collected in fluorescence mode at beamline X-11A (National Synchrotron Light Source, Brookhaven National Laboratory, Upton, NY) using a N_2-filled Stern-Heald detector and a Si(111) monochromator. Sorption samples were mounted as wet pastes in Al holders covered with Mylar windows and cooled to 77 K using a coldfinger. Reference precipitates were diluted in unreacted pyrophyllite (1 wt %) prior to analysis. At least three scans were collected for each sample. Data reduction was performed with WinXAS97 1.1 following standard procedures (*17, 18*).

Reference precipitate phases containing Ni, Al, and/or Si were synthesized using the following methods. The method of Taylor (*19*) was used to prepare Ni−Al LDH precipitates with Ni:Al 2.3:1 and 3.3:1. In addition, α-$Ni(OH)_2$ and Ni-silicate precipitates were synthesized by the methods of Genin et al. (*20*) and Grauby et al. (*21*). A nitrate-bearing Ni:Al 2.3:1 LDH was exchanged with silicate following the method of Depege et al. (*22*): 100 mL of deionized−distilled H_2O + 0.85 g of sodium metasilicate + 0.4 g of Ni−Al hydrotalcite, giving a pH of 12.2. The suspension was heated at 90 °C for 24 h under an N_2 atmosphere, and it was subsequently aged 2 weeks at 60 °C in a sealed vessel (final pH = 12.0). All solids were collected by centrifugation, washed four times with deionized−distilled H_2O, and freeze-dried.

Results and Discussion

Ni Sorption−Desorption. The partitioning of Ni from solution in a pyrophyllite suspension is shown in Figure 1A. Silica is released from the pyrophyllite structure concurrent with Ni sorption, providing evidence that the pyrophyllite surface is not stable under these experimental conditions. Aqueous Ni appears to reach equilibrium within 72 h. The reversibility of sorbed Ni decreases dramatically over the period where Ni is sequestered from solution (Figure 1B). Within a month, the fraction of Ni released from reacted solids via extraction with a 1 mM EDTA solution at pH 7.5 decreases from approximately 0.9 to 0.6. Moreover, the extraction results show that the stability of solid-phase Ni continues to increase beyond the point at which aqueous Ni reaches apparent equilibrium. These results suggest that solid-phase Ni is subject to structural transformations that are not reflected by changes in aqueous Ni solubility. To assess the validity of this hypothesis, we examined the time-dependent structural modification of the Ni surface precipitate.

Solid-Phase Characterization. An increase in the stability of the Ni surface precipitate could be attributed to several processes. First, an increase in precipitate crystallinity, via Ostwald ripening, could lead to reduced solubility (*23*). Second, chemical modifications via incorporation of ions derived from the sorbent lattice could lead to a more stable form. For example, Depege et al. (*22*) found that incorporation of silica within the interlayer of a Zn−Al LDH increased the thermal stability of the precipitate. Finally, the surface precipitate could become physically isolated from contact

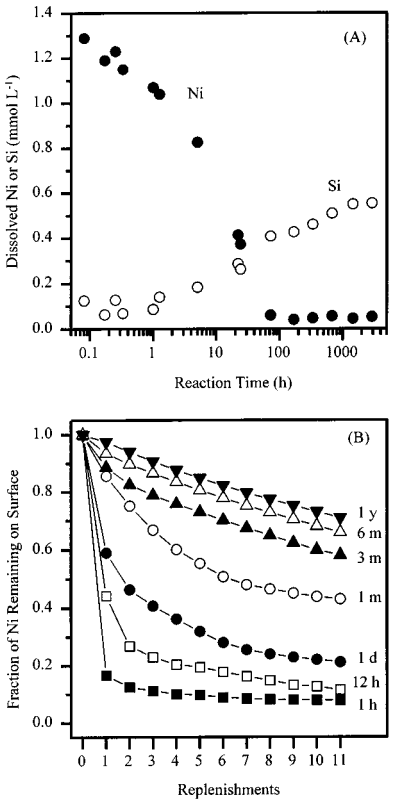

FIGURE 1. Macroscopic sorption−desorption behavior of Ni in a pyrophyllite suspension (sorption conditions: 1.5 mM Ni, 5 g L^{-1} pyrophyllite, pH 7.5). (A) The time-dependent depletion of Ni from solution and the release of Si from the pyrophyllite structure. (B) The fraction of Ni remaining on the pyrophyllite surface following extraction is plotted against the total number of EDTA extractant replenishments for a Ni-pyrophyllite aging series. The stability of solid-phase Ni increases continuously with aging time.

with solution due to precipitation of secondary Al- or Si-bearing phases during clay mineral weathering or particle coagulation. However, only the first two processes would lead to structural changes within the surface precipitate that could be detected by spectroscopic or thermal methods. To differentiate the process controlling Ni stabilization in the Ni-pyrophyllite system, we employed a suite of analytical techniques that provide complimentary data toward characterization of the Ni surface precipitate.

DRS. We used DRS in the UV−vis−NIR range to investigate Ni precipitate formation in the pyrophyllite suspension (Figure 2A). Absorption at the ν_2 band is attributed to crystal field splitting induced within the incompletely filled $3d^8$ electronic shell of Ni^{2+} through interaction with the negative charge of nearest-neighbor oxygen ions (*24*). The appearance of a Ni precipitate phase is observed within 15 min of reaction. The energy of the ν_2 spectral band is indicative of the formation of a Ni−Al LDH with Ni:Al ≅ 2:1 (Figure 2B). For comparison, the energy of ν_2 for synthetic α-$Ni(OH)_2$ and nickel phyllosilicate phases, in which Ni is the only metal within the octahedral layer, is lower, consistent with a larger Ni−O distance. The time-dependent increase in the ν_2 band intensity demonstrates the increase of the Ni precipitate up to 1 month. After 1 month there was no intensity change in ν_2, coincident with apparent equilibrium with aqueous Ni. There was a slight increase in the ν_2 energy during uptake of Ni from solution within the first week, consistent with particle growth and a decrease in the population of relaxed surface Ni octahedra (*7*). Beyond 1 week the position of ν_2 was invariant indicating that the Ni−Al octahedral layer remained unchanged throughout the course of aging.

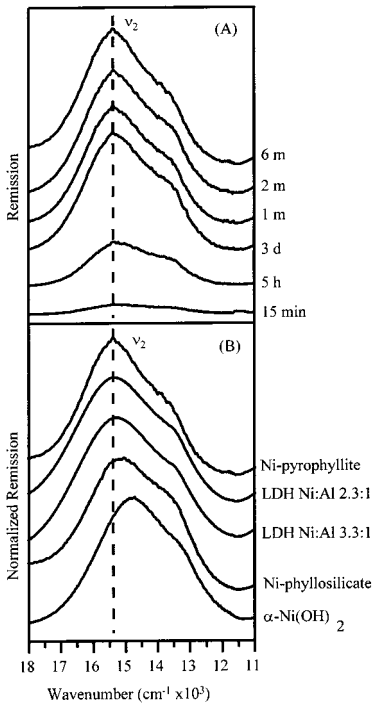

FIGURE 2. Identification and measurement of Ni surface precipitate growth using DRS to monitor the solid-phase Ni^{2+} ν_2 absorption band. (A) A series of aged Ni-pyrophyllite samples showing precipitate growth and the invariance of ν_2 energy. (B) The 1-year Ni-pyrophyllite sample and a series of reference precipitates physically mixed to 2 wt % with unreacted pyrophyllite. The position of ν_2 in Ni-pyrophyllite samples most closely matches a Ni−Al LDH.

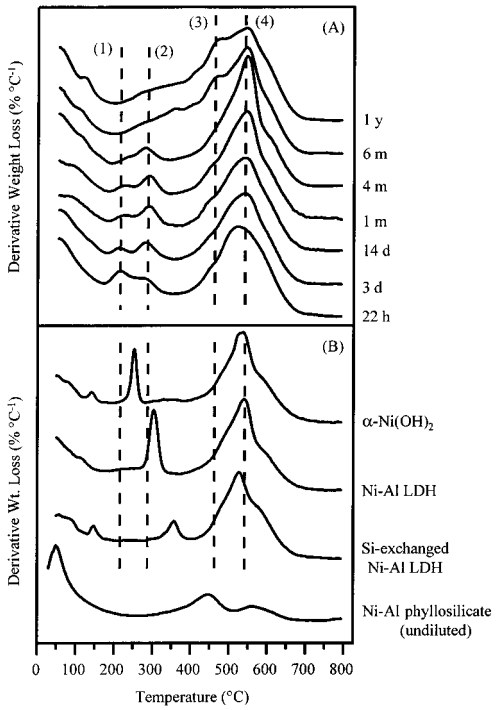

FIGURE 3. Changes in the thermal stability of the Ni surface precipitate with aging. The derivative of the weight loss curve is shown for (A) aged Ni-pyrophyllite samples and (B) reference precipitates physically diluted with pyrophyllite to match surface loading in sorption samples (2% w/w). Weight loss events: (1) expulsion of H_2O and nitrate from LDH interlayer, (2) dehydroxylation of nitrate-bearing LDH, (3) decomposition of the precursor Ni−Al phyllosilicate, and (4) dehydroxylation of pyrophyllite.

Thus, DRS failed to explain the observed increase in Ni stability up to 1 year. One possible structural modification that would not change the internal structure of the Ni−Al layer (and consequently would not change the ν_2 energy) is transformation of the Ni−Al LDH to a Ni−Al phyllosilicate via interlayer incorporation of silica derived from clay mineral weathering. Formation of a phyllosilicate structure from an LDH template is supported by research demonstrating the rapid formation of Zn− and Mg−Al phyllosilicate via hydrothermal aging of Si-exchanged Zn− and Mg−Al LDH (*22*, *25*).

HRTGA. We employed HRTGA to verify the assumption of an LDH-to-phyllosilicate transformation in Ni-pyrophyllite samples aged up to 1 year. The derivative of the weight loss for a Ni-pyrophyllite aging series is shown in Figure 3A. The temperatures of clearly distinguishable weight loss events are marked with hatched lines. The major weight loss (labeled 4) in all thermograms is due to the dehydroxylation of the pyrophyllite sorbent, occurring over the temperature range of 400−690 °C as a two-step process (*26*). Three additional weight loss events (labeled 1, 2, and 3) appear after reaction of pyrophyllite with Ni. Event 1 at about 223 °C is primarily due to expulsion of H_2O and nitrate from the interlayer (*27*, *28*). Over 4 months there is a reduction in this first weight loss which we attribute to displacement of Ni−Al LDH interlayer nitrate from increasingly available aqueous silica, which derives from weathering of the pyrophyllite structure. The second weight loss is due to dehydroxylation of the octahedral layer and complete collapse of the LDH structure (*28*). This decomposition temperature (labeled 2) remains at approximately 284 °C over 4 months. For the 6 month and 1 year samples, however, this weight-loss event is shifted toward higher temperature and occurs as a shoulder on the larger pyrophyllite dehydroxylation event at approximately 462 °C (labeled 3).

The observed shift in decomposition temperature is too large to be explained solely by an increase in the crystallinity of the Ni−Al LDH surface precipitate (*29*). To investigate the source of this shift, we compared the weight-loss temperatures of the Ni-reacted samples with those of physical mixtures of pyrophyllite with reference Ni compounds (Figure 3B). The median dehydroxylation temperature of the Ni−Al LDH sample at 304 °C is slightly higher than the one observed for the Ni-reacted samples within the first 4 months. However, a modification of this sample by exchanging silica for the interlayer nitrate coupled with hydrothermal aging (*22*) shifted the dehydroxylation temperature to 357 °C (Figure 3B). Displacement of interlayer nitrate of this sample was confirmed via infrared spectroscopy by a reduction in absorbance for the nitrate asymmetric stretch (ν_3) centered at 1380 cm^{-1} (not shown). In addition, the appearance of Si−O and Si−O−Si vibrational bands at 1010 and 855 cm^{-1} (not shown) for the Si-exchanged synthetic Ni−Al LDH demonstrated the incorporation and polymerization of Si within the interlayer (*22*).

For comparison, the dehydroxylation of an undiluted synthetic Ni−Al phyllosilicate is shown in Figure 3B. The undiluted sample decomposes at a temperature very similar to that observed for the sorption samples aged for 6 months or longer. However, the decomposition of the synthetic Ni−Al phyllosilicate could not be distinguished when physically mixed with pyrophyllite even at a weight percent twice the surface loading in sorption samples (∼2%). Thus, the additional weight loss at 462 °C in aged sorption samples may be due to the release of entrapped H_2O or nitrate within the interlayer. This indicates that Si has not formed a uniform tetrahedral sheet bound to the Ni−Al octahedral layer. Therefore, the surface precipitate in samples collected beyond 1 month appears to be an evolving precursory form of a Ni−Al phyllosilicate.

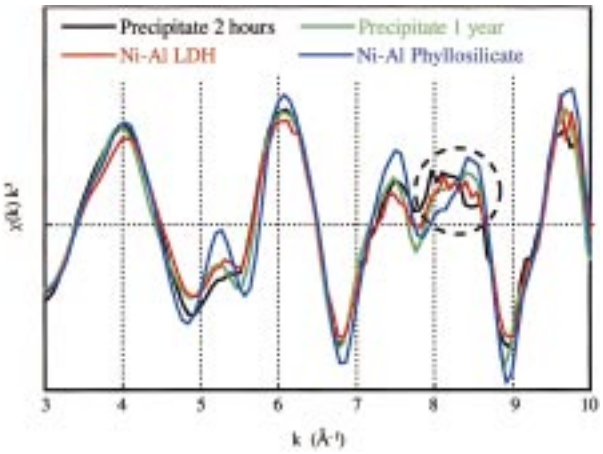

FIGURE 4. Normalized and weighted Ni K-edge EXAFS spectra, $\chi(k)k^3$, for a reference Ni−Al LDH and Ni−Al phyllosilicate and the Ni surface precipitate formed on pyrophyllite at 2 h and 1 year. The characteristic oscillations between 8 and 9 $Å^{-1}$ indicate partial transformation from a Ni−Al LDH to a Ni−Al phyllosilicate.

EXAFS. This interpretation is supported by comparison of EXAFS data collected for reference Ni−Al LDH and Ni−Al phyllosilicate precipitates and sorption samples collected at 2 h and 1 year (Figure 4). The normalized and weighted Ni K-edge EXAFS spectra, $\chi(k)k^3$, are very similar in phase and amplitude over the k-range 3−10 A^{-1}. However, there is a noticeable difference in the scattering amplitude within the region 8−9 A^{-1}, where backscattering of the Ni photoelectron is sensitive to the presence of second-shell Al within the octahedral layer and tetrahedral Si attached to Ni via a corner-sharing bond (*30*, *31*). The enhanced upward oscillation at ~8.5 $Å^{-1}$ in the 1 year Ni-pyrophyllite is consistent with attachment of a fraction of the exchanged interlayer Si to the Ni−Al octahedral sheet. Thus, the structure of the Ni surface precipitate at 1 year appears to be intermediate between that of Ni−Al LDH and Ni−Al phyllosilicate.

Charlet and Manceau (*32*) propose that a layered Ni silicate forms at the clay mineral surface during sorption, with Ni as the sole metal within the octahedral layer. This conclusion is based on two observations from EXAFS analysis: (1) contraction of the nearest-neighbor Ni−Ni bond distance relative to that found in β-$Ni(OH)_2$ and (2) evidence for a corner-sharing bond between Ni octahedra and Si tetrahedra. Both structural features are generally observed in trioctahedral phyllosilicates (*33*). In contrast, we have provided definitive evidence that a Ni−Al LDH is the initial precipitate that forms during sorption to Al-bearing clay minerals (*7*). This observation is unexpected since Ni phyllosilicates, e.g., nepouite or pimelite, are more common in certain soil environments, while the structurally related Ni−Al LDH precipitates have remained undetected (*34*). Our detection of an intermediate phase provides a possible explanation: the LDH precipitate is only metastable and transforms toward a phyllosilicate in the presence of soluble silica derived from soil minerals (*35*).

Formation of a *fully* crystallized Ni−Al phyllosilicate is not required to induce increased thermal stability or resistance to dissolution. The formation of even a small percentage of silica tetrahedral or polyhedral bonds between hydroxide sheets is expected to impart measurable stability to the layered structure. During dissolution, this will prevent the total delamination of octahedral layers, and resultant surface area increase, that would likely occur in an LDH in which weakly bound nitrate occupies the interlayer. Thus, we anticipate that the structural stability of the surface precipitate would continue to increase with time as a fully attached silica sheet develops.

We hypothesize that the observed stabilization is realized through exchange of silica for nitrate within the Ni−Al LDH interlayer leading to formation of a precursor Ni−Al phyllosilicate. Our results suggest that under certain conditions Ni removal from solution in pyrophyllite suspensions proceeds via at least two steps: (1) initial formation of a Ni−Al LDH precipitate where Al is derived from the pyrophyllite structure and (2) the ultimate formation of a Ni−Al phyllosilicate due to incorporation of Si (derived from the pyrophyllite) into the Ni−Al LDH interlayer. This latter process can be viewed as a silication of the LDH structure.

These results suggest that formation of a Ni−Al LDH phase is a necessary intermediate step toward formation of more stable Ni-Al phyllosilicate-type phases in Al-bearing clay mineral systems. The overall rate of phyllosilicate formation will be tied to the stability of the soil clay mineral assemblage as well as the relative concentration of anions that may compete for the LDH interlayer space. The stabilization pathway elucidated in this study is significant toward evaluation of the long-term mobility of Ni and other transition metals in soils. Clearly, inadequate assessments may result if the influence of mineral (or sorbent) weathering is not considered in modeling sorption reactions at the mineral−water interface.

Acknowledgments

Supported by grants from the USDA-NRI Program, the DuPont Company, and the Delaware Research Partnership Program. Brian McCandless (Institute of Energy Conversion, University of Delaware) provided access to the UV−vis−NIR spectrophotometer. This manuscript benefited from comments by E. Elzinga and constructive, anonymous reviews.

Literature Cited

(1) Stumm, W. *Chemistry of the Solid-Water Interface*; John Wiley & Sons: New York, 1992.
(2) Sparks, D. L. *Environmental Soil Chemistry*; Academic Press: San Diego, 1995; Chapter 5.
(3) Davis, J. A.; Kent, D. B. In *Mineral-Water Interface Geochemistry*; Hochella, M. F., Jr., White, A. F., Eds.; Mineralogical Society of America: Washington, DC, 1990; Vol. 23, pp 177−260.
(4) d'Espinose de la Caillerie, J.-B.; Kermarec, M.; Clause, O. *J. Am. Chem. Soc.* **1995**, *117*, 11471.
(5) Towle, S. N.; Bargar, J. R.; Brown, G. E., Jr.; Parks, G. A. *J. Colloid Interface Sci.* **1997**, *187*, 62.
(6) Scheidegger, A. M.; Lamble, G. M.; Sparks, D. L. *J. Colloid Interface Sci.* **1997**, *186*, 118.
(7) Scheinost, A. C.; Ford, R. G.; Sparks, D. L. *Geochim. Cosmochim. Acta* **1999**, in press.
(8) Elzinga, E. J.; Sparks, D. L. *J. Colloid Interface Sci.* **1999**, *213*, 506.
(9) Bish, D. L.; Brindley, G. W. *Am. Mineral.* **1977**, *62*, 458.
(10) Cavani, F.; Trifiro, F.; Vaccari, A. *Catal. Today* **1991**, *11*, 173.
(11) Scheidegger, A. M.; Strawn, D. G.; Lamble, G. M.; Sparks, D. L. *Geochim. Cosmochim. Acta* **1998**, *62*, 2233.
(12) O'Day, P. A.; Chisholm-Brause, C. J.; Towle, S. N.; Parks, G. A.; Brown, G. E., Jr. *Geochim. Cosmochim. Acta* **1996**, *60*, 2515.
(13) Nowack, B.; Sigg, L. *J. Colloid Interface Sci.* **1996**, *177*, 106.
(14) Borggaard, O. K. *Z. Pflanzenernahr. Bodenk.* **1992**, *155*, 431.
(15) Bryce, A. L.; Kornicker, W. A.; Elzerman, A. W.; Clark, S. B. *Environ. Sci. Technol.* **1994**, *28*, 2353.
(16) Bryce, A. L.; Clark, S. B. *Colloids Surf.* **1996**, *107*, 123.
(17) Ressler, T. *J. Phys. IV* **1997**, *7*, 269.
(18) Brown, G. E., Jr.; Calas, G.; Waychunas, G. A.; Petiau, J. In *Spectroscopic Methods in Mineralogy and Geology*; Hawthorne, F. C., Ed.; Mineralogical Society of America: Washington, DC, 1988; Vol. 18, pp 431−512.
(19) Taylor, R. M. *Clay Miner.* **1984**, *19*, 591.
(20) Genin, P.; Delahaye-Vidal, A.; Portemer, F.; Tekaia-Elhsissen, K.; Figlarz, M. *Eur. J. Solid State Inorg. Chem.* **1991**, *28*, 505.
(21) Grauby, O.; Petit, S.; Decarreau, A.; Baronnet, A. *Eur. J. Mineral.* **1993**, *5*, 623.
(22) Depege, C.; el Metoui, F.-Z.; Forano, C.; de Roy, A.; Dupuis, J. *Chem. Mater.* **1996**, *8*, 952.
(23) Morse, J. W.; Casey, W. H. *Am. J. Sci.* **1988**, *288*, 537.

(24) Burns, R. G. *Mineralogical Applications of Crystal Field Theory*; Cambridge University Press: Cambridge, 1993.
(25) Schutz, A.; Biloen, P. *J. Solid State Chem.* **1987**, *68*, 360.
(26) Evans, B. W.; Guggenheim, S. In *Hydrous Phyllosilicates (Exclusive of Micas)*; Bailey, S. W., Ed.; Mineralogical Society of America: Washington, DC, 1988; Vol. 19, pp 225−294.
(27) Pesic, L.; Salipurovic, S.; Markovic, V.; Vucelic, D.; Kagunya, W.; Jones, W. *J. Mater. Chem.* **1992**, *2*, 1069.
(28) Bellotto, M.; Rebours, B.; Clause, O.; Lynch, J.; Bazin, D.; Elkaim, E. *J. Phys. Chem.* **1996**, *100*, 8535.
(29) Carriat, J. Y.; Che, M.; Kermarec, M. *Catal. Lett.* **1994**, *25*, 127.
(30) Manceau, A. *Can. Mineral.* **1990**, *28*, 321.
(31) Scheinost, A. C.; Sparks, D. L., submitted for publication in *J. Colloid Interface Sci.*
(32) Charlet, L.; Manceau, A. *Geochim. Cosmochim. Acta* **1994**, *58*, 2577.
(33) Bailey, S. W. In *Micas*; S. W. Bailey, Ed.; Mineralogical Society of America: Washington, DC, 1984; Vol. 13, pp 13−60.
(34) Uren, N. C. In *Advances in Agronomy*; Sparks, D. L., Ed.; Academic Press: San Diego, 1992; Vol. 48, pp 141−203.
(35) Iler, R. K. *The Chemistry of Silica*; John Wiley & Sons: New York, 1979.

Received for review March 10, 1999. Revised manuscript received June 28, 1999. Accepted July 6, 1999.

ES990271D